J. Anal. Appl. Pyrolysis 86 (2009) 215–220

Contents lists available at ScienceDirect

Journal of Analytical and Applied Pyrolysis

journal homepage: www.elsevier.com/locate/jaap

H-ZSM-11 and Zn-ZSM-11 zeolites and their applications in the catalytic transformation of LDPE

María S. Renzini [a,1], Ulises Sedran [b,1], Liliana B. Pierella [a,1,*]

[a] Grupo Zeolitas, CITeQ (Centro de Investigación y Tecnología Química), Facultad Córdoba, Universidad Tecnológica Nacional, Córdoba, Argentina
[b] INCAPE (FIQ, UNL – CONICET), Santiago del Estero 2654, (S3000AOJ) Santa Fé, Argentina

ARTICLE INFO

Article history:
Received 5 January 2007
Accepted 28 June 2009
Available online 5 July 2009

Keywords:
LDPE
Thermal and catalytic degradation
ZSM-11
Aromatics

ABSTRACT

Low density polyethylene was converted into hydrocarbons over Zn- and H-ZSM-11 zeolite catalysts in a fixed-bed reactor during 20 and 60 min reaction time, 0.5 and 2.0 polymer to catalyst mass ratio at 500 °C. The zeolites were synthesized by conventional techniques and characterized by XRD, pyridine FTIR and N_2 adsorption. The adsorbed pyridine spectra demonstrated that new Lewis sites were formed after Zn exchange, and that the relationship between Lewis and Brönsted sites in the Zn-ZSM-11 zeolite (3.53) was much higher than that in the H-ZSM-11 zeolite (0.09). Thermal analyses confirmed that the temperature of decomposition of the polymer can be decreased in as much as about 145 °C when the catalysts were added. As compared to the thermal degradation, the catalytic conversion produced less solid residues and much higher amounts of gas and liquid hydrocarbons. The catalysts showed different yield profiles: the H-ZSM-11 zeolite yielded more gases, while the Zn-ZSM-11 zeolite yielded more liquid products. Notably over Zn-ZSM-11 zeolite, these liquid products were mainly aromatic, and depending on experimental conditions (higher temperature, longer reaction time, smaller polymer/catalyst relationship), aromatic selectivity could be increased to almost 100%.

1. Introduction

Due to their versatility and low cost, the use of plastic goods had an exponential increase over the past few decades. Among the most used plastics, polyolefins such as polyethylene and polypropylene have a massive production and consumption in a large number of applications such as packaging, building, electricity and electronics, agriculture, health care, etc. [1]. Particularly, low density polyethylene (LDPE) is employed in packaging containers, dispensing bottles, wash bottles, tubing and plastic bags [2].

With an annual consumption of nearly 100 kg of plastic per person [3], the management of the resulting vast waste stream represents a matter of great social and environmental concern, and the recycling of waste polymers is a requirement to mitigate their impact on the environment [4]. Among various alternatives, the direct reprocessing (primary recycling), that can only be applied up to a certain limit, the use of biodegradable polymers, the controlled incineration for the recovery of energy, or thermal pyrolysis processes that produce a wide spectrum of hydrocarbons [5,6], have been considered. The main conventional methods of final disposition, i.e., land filling and incineration (secondary recycling), pose a number of problems and do not have wide acceptance.

However, various tertiary recycling processes are attractive, since they produce valuable chemicals or fuels [7], and during the last decades numerous studies have been devoted to processes of waste polymer degradation with that aim [8–10]. The tertiary recycling of polyolefins (particularly polyethylene) has been attempted under different approaches [11,12]. As compared to thermal processes, the use of catalysts for the transformation of polyethylene yields a much narrower product distribution, and the temperature of the process can be reduced to the range of 350–550 °C. Many examples can be found in the literature in relation to the catalytic degradation of this polyolefin employing solid acid zeolites, amorphous silica–aluminas and mesoporous materials such as MCM-41 [13–16].

It is known that the thermal degradation of polyethylene occurs through the radical random-chain scission mechanism, with a wide spectrum of hydrocarbon products [17]. On the other hand, the catalytic degradation of polyethylene is known to proceed by a carbenium ion mechanism [18]. The initial steps are considered to occur by either the abstraction of a hydride ion from the polyethylene chain by Lewis acid sites or the addition of a proton to the C–C bonds in the polymer by Brönsted acid sites. Successive scission of the main chains occurs to produce fragments that are further cracked or dehydrocyclized in the subsequent steps [19].

* Corresponding author.
E-mail addresses: lpierella@scdt.frc.utn.edu.ar, lpierella@gmail.com (L.B. Pierella).
[1] CONICET, Argentina.

0165-2370/$ – see front matter © 2009 Elsevier B.V. All rights reserved.
doi:10.1016/j.jaap.2009.06.008

It is the main objective of this work to investigate the catalytic performance of medium pore size ZSM-11 zeolites (MEL structure), both in its protonic form and modified with Zn^{2+}, in the degradation of LDPE, as well as the influence of the reaction time and the polymer to catalyst ratio on the product distribution. In addition, the comparative analysis with the results of a thermal degradation process was performed.

2. Experimental

2.1. Catalyst preparation

The parent Na-ZSM-11 zeolite (Si/Al = 17) was obtained by known methods of hydrothermal crystallization, using tetrabutylammonium hydroxide as a structure directing agent [20]. The ammonium form of the zeolite (NH_4-zeolite) was prepared by ion exchange of the as-prepared Na-zeolite form with 1 M ammonium chloride solution at 80 °C for 40 h. The Zn-zeolite form with 2.83 wt.% of Zn was obtained by ion exchange of the NH_4-zeolite with 0.5 M zinc nitrate solution by refluxing during 20 h at 100 °C. Finally, the NH_4-zeolite and the Zn-zeolite materials were dried at 110 °C, treated in a nitrogen flow at 500 °C during 8 h and then calcined in air at same temperature for 10 h just prior to use, obtaining the H-ZSM-11 and the Zn-ZSM-11 catalysts, respectively.

2.2. Catalyst characterization

The pentasil MEL materials were characterized by different techniques. The zinc effective content of the Zn-ZSM-11 catalyst was determined by atomic absorption spectrometry in a Perkin Elmer AAnalyst 800 spectrometer after microwave digestion of the sample in a Milestone ETHOS 900 digester.

X-ray powder diffraction (XRD) patterns were collected in air at room temperature in a Phillips PW-1700 equipment, using Cu Kα radiation of wavelength 1.54 Å. Diffraction data were recorded from 5–60° 2-theta angles, with an interval of 0.01° and scanning rate of 2°/min.

Infrared analyses were performed in a JASCO 5300 FTIR spectrometer. For structure characterization in the lattice vibration region (400–1800 cm^{-1}), the samples were mixed with KBr at 0.05% and pressed forming wafers. In order to determine the type and concentration of acidic sites, pyridine (Py) adsorption experiments were carried out on the H-ZSM-11 and Zn-ZSM-11 catalysts using self-supporting wafers (8–10 mg cm^{-2}) in a thermostatized cell with CaF_2 windows connected to a vacuum line. Pyridine (3 Torr) was adsorbed at room temperature and desorbed at 400 °C and 10^{-4} Torr for an hour. The numbers of Brönsted and Lewis acid sites were calculated from the maximum intensity of the adsorption bands at 1545 cm^{-1} and 1450–1460 cm^{-1}, respectively, and quantified using the literature data of the integrated molar extinction coefficients [21], which are independent of the catalysts or strength of the sites.

The assessment of the specific surface areas by the BET method was carried out with N_2 adsorption at 77 K using a Micromeritics ASAP 2000 equipment.

2.3. Feed characterization

The reactant pure LDPE was analyzed by FTIR (JASCO 5300) and XRD (Phillips PW-1700) using Cu Kα radiation of wavelength 1.54 Å. Diffraction data were recorded from 5–40° 2-theta angles and scanning speed of 2°/min. The thermal degradation of LDPE alone and mixed with the catalysts was investigated using a thermal analysis instrument (TA Instruments 2950 TGA and 2920 MDSC). Samples were subjected to a constant heating rate of 10 °C/min from room temperature to 550 °C under flow of nitrogen of 50 ml/min.

2.4. Catalytic activity

The experiments of LDPE conversion were performed in a fixed-bed, quartz tubular reactor, with an inner diameter of 9 mm and a length of 300 mm, operating at atmospheric pressure. The reactor was continuously purged with nitrogen as carrier gas with a flow of 25 ml/min. Both the thermal (no catalyst added) and catalytic degradation of LDPE were carried out with a heating rate of 25 °C/min from room temperature to 500 °C and held at this temperature for 20 and 60 min, respectively. The reactor bed comprised a bottom layer of quartz particles, then the catalyst and finally the LDPE pellets, with approximately 0.5 cm average size.

The reactor was connected to an ice-salt condenser to collect any condensable liquid product, followed by a gas collection bag to collect volatile products. After each experiment, the catalyst was removed from the reactor and the amount of coke was determined by the difference in weight before and after regeneration in air at 500 °C for 10 h. The total liquid yield was assessed by difference in the condenser system weight before and after the experiment. The amount of gas products was determined by means of an overall mass balance of the experiment. The products were analyzed using a HP5890 gas chromatograph equipped with a FID detector. The liquid hydrocarbons were analyzed using a HP-1 capillary column (30 m, 0.32 mm i.d., 2.65 μm phase thickness) and the gaseous products in a Porapak Q packed column (2.2 m, 2 mm i.d.). Gas chromatography/mass spectrometry (Shimadzu GC-17A, QP5050) was used for the identification of products, using a 25 m, 0.2 mm i.d. HP-5 capillary column.

3. Results and discussion

It can be seen in Table 1 that the total surface areas of H-ZSM-11 and Zn-ZSM-11 catalysts are very similar. Crystallinity, as assessed from both XRD and FTIR techniques is very high, thus confirming that the severe conditions employed during the chemical and thermal treatments did not affect the structural characteristics of the catalysts.

Fig. 1 shows that the signals characteristic of the parent Na-ZSM-11 catalyst are observed at 2θ angles of 23–24° and 7–9°, which do not alter after the incorporation of Zn^{2+} and H^+ cations.

The FTIR spectra of pyridine adsorbed on H-ZSM-11 and Zn-ZSM-11 catalysts are shown in Fig. 2 (1400–1700 cm^{-1} zone). An intense band can be seen at 1636 cm^{-1} which is assigned to structural OH^- ion vibration [22] indicative of the interaction of pyridine with Brönsted acid sites (PyH^+), the intensity being higher in the H-ZSM-11 catalyst; this material also presents a signal at 1620–1623 cm^{-1}, related to pyridine interaction with Lewis acid sites (PyL) of the framework aluminum [23]. The Zn-ZSM-11 catalyst presents an intense signal at 1616 cm^{-1} that could be related to new Lewis acid sites (electron donor–acceptor, EDA) generated by the zinc incorporation [20,24]. The position of the bands close to 1600 cm^{-1} can be considered as an indication of the Lewis acid strength of the surface sites [25]. Bands at higher wavenumbers (1620–1623 cm^{-1}) would result from strong Lewis

Table 1
Catalyst surface area and crystallinity.

Catalysts	Surface area (m^2/g)	Crystallinity (%)	
	BET	XRD	FTIR[a]
H-ZSM-11	392	100	>99
Zn-ZSM-11	378	>98.5	>97

[a] FTIR in the fingerprint zone of the MEL materials (400–1400 cm^{-1}).

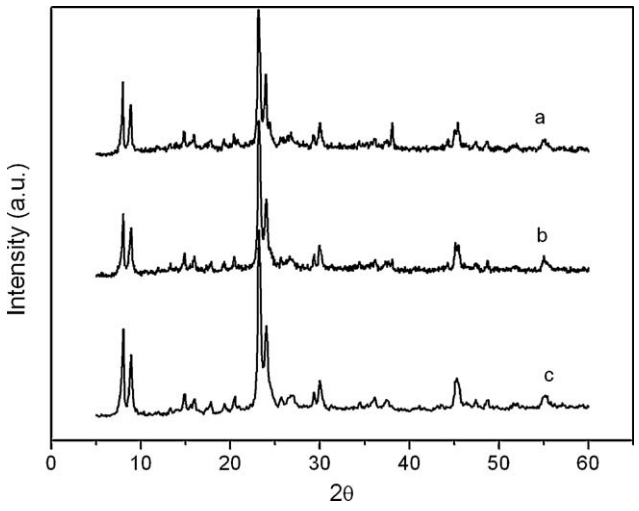

Fig. 1. XRD patterns of the catalysts: (a) H-ZSM-11; (b) Zn-ZSM-11; (c) matrix Na-ZSM-11.

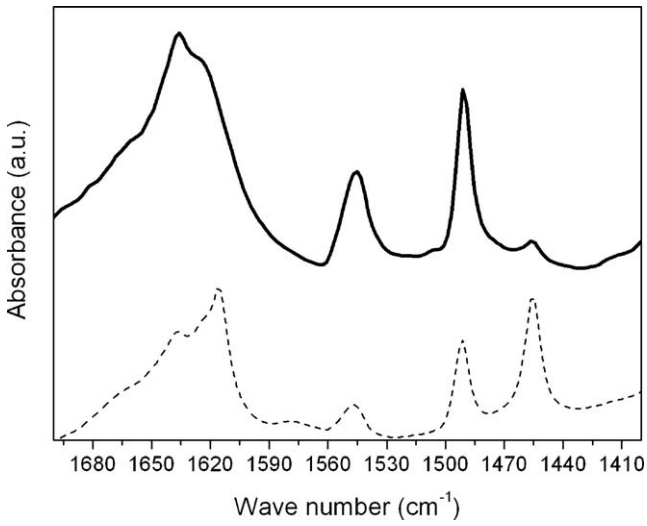

Fig. 2. FTIR spectra of pyridine adsorbed on the catalysts. Full line: Zn-ZSM-11 and dashed line: H-ZSM-11.

sites whereas bands at lower wavenumbers (1616 cm^{-1}) would indicate medium to strong sites [22].

Bands at 1455, 1490 and 1545 cm^{-1} can be observed in both cases. The band at 1490 cm^{-1} corresponds to the vibration of pyridine adsorbed over Brönsted and Lewis acid sites [26,27]. Bands at 1455 cm^{-1}, corresponding to PyL, as well as bands at 1545 cm^{-1}, indicative of the PyH^+ interaction, can be observed. The H-ZSM-11 catalyst spectrum shows an important signal of PyH^+ sites at 1545 cm^{-1} and a less important PyL signal resulting from Al^{3+} sites. The introduction of zinc cations to obtain the Zn-ZSM-11 catalyst caused a significant decrease in the intensity of the PyH^+ band at 1545 cm^{-1}, thus confirming that some of the zeolite protons are consumed during the exchange process with the zinc solution [28]. The formation of new EDA adducts of PyL sites at 1455 cm^{-1} is clear in the strong enhancement of that band [22]. Upon zinc introduction, the total number of acid sites increased and, consistently with the observations, the Lewis to Brönsted ratio was significantly augmented (0.09 for H-ZSM-11 and 3.53 for Zn-ZSM-11 catalysts, respectively, see Table 2).

Table 2
Catalyst acid properties by pyridine FTIR.

Catalyst	Brönsted (mmol Py/mg)	Lewis (mmol Py/mg)	Total acid sites (mmol Py/mg)	Lewis/Brönsted
H-ZSM-11	0.0133	0.0012	0.0145	0.09
Zn-ZSM-11	0.0046	0.0163	0.0209	3.53

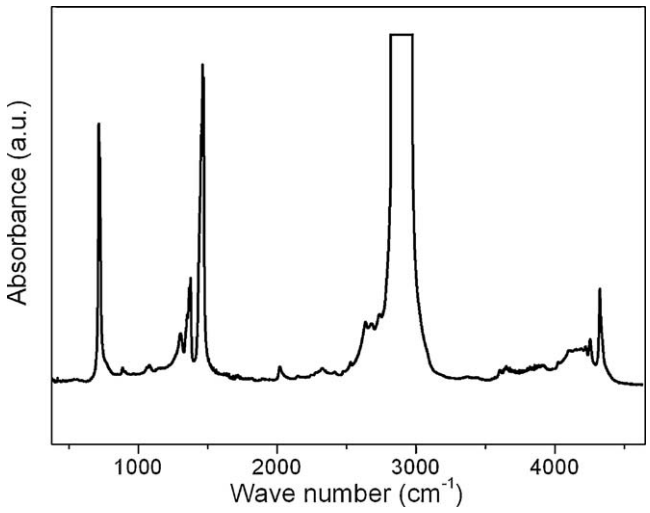

Fig. 3. FTIR spectra of LDPE.

The pure LDPE employed in this study was characterized by FTIR and XRD techniques. Fig. 3 presents the FTIR spectrum of LDPE, showing characteristic bands at 721 and 1470 cm^{-1} that correspond to the rocking and bending vibration of CH_2 groups, respectively, and the strong absorption bands at 2850–2941 cm^{-1} which represent the CH_2 stretching [29]. The characteristic X-ray diffraction signals of the LDPE are shown in Fig. 4; there are two sharp peaks in the pattern at $2\theta = 21^\circ$ and $2\theta = 24^\circ$, which are assigned to the 110 and 200 reflections of the orthorhombic subcell, respectively, similar to the observations reported by Chen et al. [30].

Fig. 5 shows the results of the thermal analysis (DSC) of the pure LDPE and a 0.5/1 LDPE/catalyst physical mixture. An endothermic signal at 112 °C can be related to the melting point of LDPE, which is consistent with published data [31,32]; a peak corresponding to the thermal decomposition of pure LDPE can be observed at 473 °C. The LDPE decomposition temperature was lowered significantly in the presence of the catalysts. The decrease in the decomposition temperature was larger for the H-ZSM-11 material (327 °C) than for the Zn-ZSM-11 catalyst (341 °C), a fact that may be related to the higher amount of Brönsted sites in the H-zeolite in respect to the Zn-zeolite (see Table 2 and Fig. 2), that favors the initial cracking.

Table 3 shows the influence of the reaction time on the liquid and gaseous hydrocarbon product yields and solid residues yield for the thermal and catalytic degradation of LDPE at 500 °C and polymer to catalyst ratio of 0.5. The production of solid residues in the thermal cracking corresponded mainly to waxes adhered in the walls of the reactor, coke yield being minimum. It can be seen that increasing the reaction time from 20 to 60 min in the thermal degradation process results in higher yields of gaseous and liquid products in detriment of solid residues. This expected result is consistent with those reported by Mosio-Mosiewski et al. [33].

An increase in reaction time in the experiments with both H-ZSM-11 and Zn-ZSM-11 catalysts enhanced the yield of gaseous products and solid residues and decreased the yield of liquids. This behavior may be explained by the over-cracking promoted by the combined effects of the temperature and time of reaction.

The distribution of reaction products in the experiments with catalysts are shown in Table 4. The H-ZSM-11 catalyst produced a

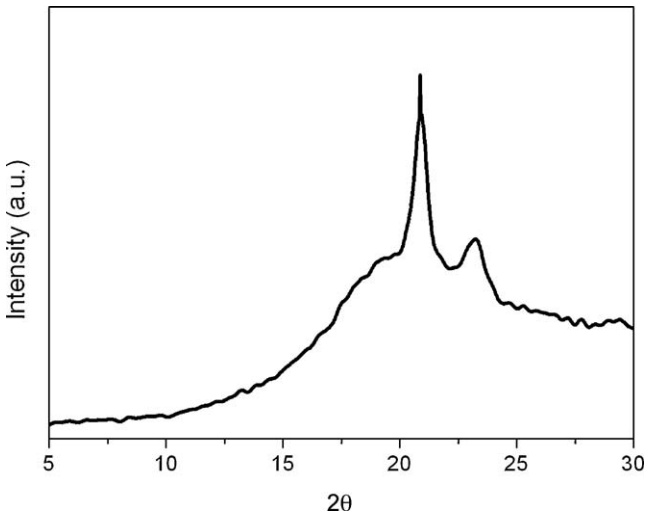

Fig. 4. XRD pattern of LDPE.

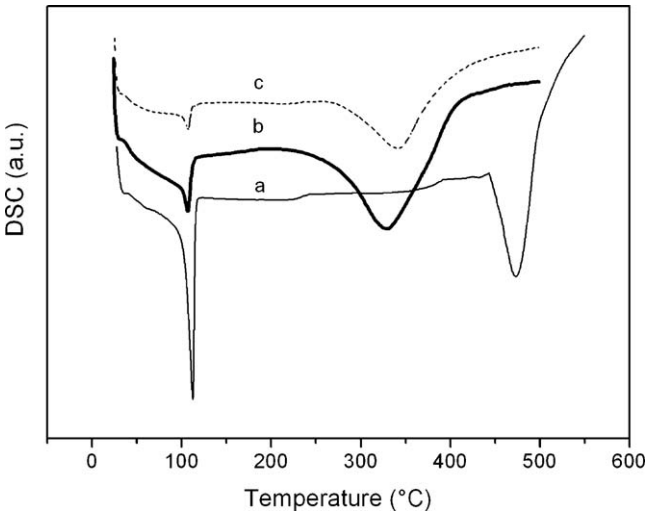

Fig. 5. DSC of pure LDPE and 0.5/1 physical mixtures of LDPE/catalyst: (a) pure LDPE; (b) LDPE/H-ZSM-11; (c) LDPE/Zn-ZSM-11.

higher amount of gaseous hydrocarbons, with an important proportion of liquefied petroleum gas (LPG, C3–C4). On the contrary, the Zn-ZSM-11 catalyst produced large quantities of liquid hydrocarbons with high yields of aromatic compounds in the C6–C9 range (benzene, toluene, xylenes, trimethylbenzenes, ethyltoluene and ethylbenzene), while the C5–C6 fractions were smaller. These facts may be explained by the known selective formation of aromatics over Lewis acid sites by a combination of cyclization and hydrogen transfer processes [34]. Note that the Zn-ZSM-11 catalyst has a much higher proportion of Le sites than H-ZSM-11 catalyst (see Table 2). The direct aromatization of C6 and larger fragments, and the oligomerization and cyclization of C4–C5 fragments in polyethylene cracking had been also postulated by Takuma et al. [35]. On the contrary, the reactions over H-Zeolite showed more cracking products from both the classic β-cracking mechanism and the proteolysis of pentacoordinated carbonium ions, according to the larger amounts of Brönsted sites present in this sample (see Table 2) [36–39]. Among the LPG hydrocarbons, the proportion of olefins higher, close to 31%, with the Zn-ZSM-11 catalyst at the shortest reaction time. Longer reaction times promoted the degradation of liquid, resulting in an increase in the yield of the gaseous fractions. The distribution of liquid products shifted to lower carbon numbers per molecule in the products, with almost complete disappearance of the non-aromatic $C7^+$ and polycyclic aromatic fractions that were observed over both catalysts at shorter reaction times. The yields of coke and their impact on catalyst stability will be examined in more detail in an additional study.

Table 3
Influence of the reaction time on the yields of the main products for the thermal and catalytic degradation of LDPE. Reaction temperature, 500 °C and polymer/catalyst relationship, 0.5.

Catalyst	Reaction time (min)	Gas (wt.%)	Liquid (wt.%)	Residues (wt.%)
No catalyst	20	11.94	6.36	81.70
	60	24.38	18.72	56.90
Zn-ZSM-11	20	16.95	81.77	1.28
	60	40.06	55.12	4.82
H-ZSM-11	20	39.00	57.01	3.99
	60	62.51	30.56	6.93

Table 4
Product distribution of the LDPE catalytic degradation at different reaction times. Reaction temperature, 500 °C and polymer/catalyst relationship, 0.5.

Product (wt.%)	Catalyst			
	Zn-ZSM-11		H-ZSM-11	
	20 min	60 min	20 min	60 min
C1–C2	1.59	4.85	5.14	2.47
C3–C4 olefins	3.81	7.75	2.89	14.49
C3–C4 paraffins	8.39	22.75	20.73	33.79
C5	6.90	3.02	14.01	11.57
C6	4.31	1.68	1.76	1.34
C6–C9 Aromatics	35.83	52.98	25.38	26.88
C7–C8	15.25	1.20	10.50	0.00
C9–C10	8.71	0.94	6.00	2.53
C11–C16	10.71	0.00	7.38	0.00
Polyciclic aromatics	3.22	0.00	2.22	0.00

The impact of the different relationships between the masses of polymer and catalyst was studied with the Zn-ZSM-11 zeolite and shown in Fig. 6. The DTG analysis shows that, as long as the catalyst mass was increased, the decrease in the decomposition temperature of the polymer was very significant. As previously shown (refer to Fig. 5), the addition of this catalyst to the polymer decreased the polymer decomposition temperature in more than 140 °C and more than 75 °C for the polymer to catalyst relationships of 0.5 and 2, respectively. Particularly, a shoulder can be observed at lower temperatures in the lowest relationship profile that reveals the existence of at least two different stages in the catalytic degradation of LDPE. The first stage could be assigned to a pre-cracking of the polymer, probably occurring at the external acid sites in the zeolite, the second one consisting in the cracking of the oligomers formed at the initial stage, and probably occurring in the internal acid sites, inside the pore system of the zeolite.

The gas, liquid and coke yields also changed as a function of the polymer to catalyst relationships, results being shown in Table 5 for the Zn-ZSM-11 catalyst. It is to be noted that no polymer was observed left on the catalyst or reactor walls after the reaction, indicating that conversion was complete under the conditions tested. Only coke was noticed on the catalyst. A higher liquid yield was observed at a polymer/catalyst ratio of 2, the addition of more catalyst having an adverse effect. Indeed, it was observed in the experiments with lower polymer/catalyst ratios (0.5), that cracking of the products into smaller molecules collected in the gaseous fraction occurred, as was also reported by Akpanudoh et al. [40]. Particularly, the LPG fraction was the most important among gases. The increase in the Lewis active sites generated by

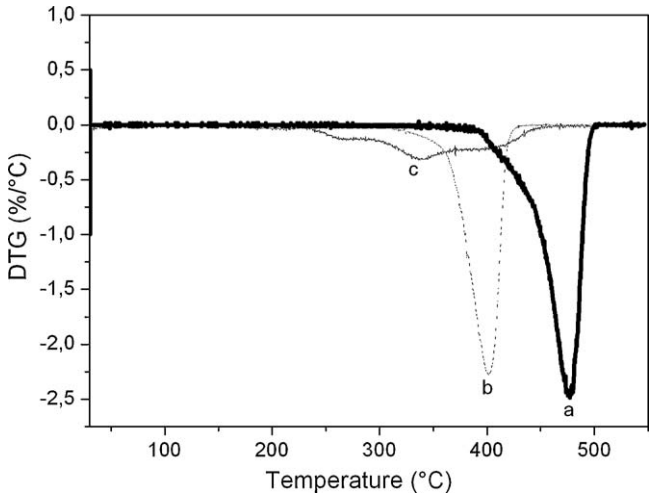

Fig. 6. DTG analysis of pure LDPE and physical mixtures of LDPE/Zn-ZSM-11 catalyst: (a) pure LDPE; (b) LDPE/Zn-ZSM-11, relationship 2; (c) LDPE/Zn-ZSM-11, relationship 0.5.

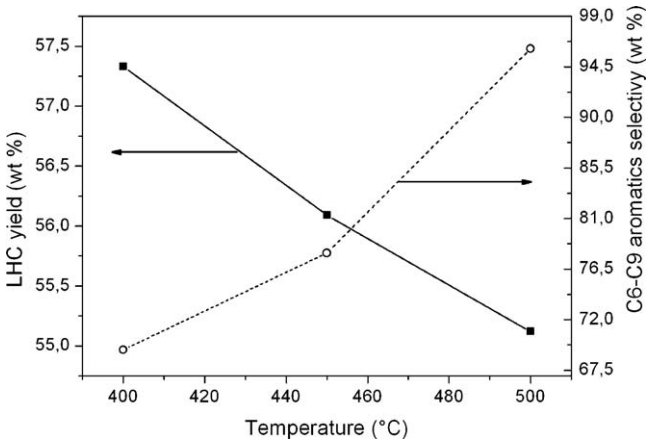

Fig. 7. Effect of reaction temperature on the yields of C6–C9 aromatics. Reaction time, 60 min; polymer/catalyst ratio 0.5.

the incorporation of zinc and the shape selectivity properties of the zeolite promoted the significantly high production of C6–C9 aromatic hydrocarbons, which in the case of the smallest plastic/catalyst relationship was close to 53%, representing a very high proportion of above 96% of aromatics in the liquid fraction. A much smaller proportion of C6–C9 aromatics (18% of the liquid fraction) was observed at a polymer/catalyst ratio of 2, and a consequent overall increase in aliphatic C6–C10 hydrocarbons can be noticed. These trends in the aromatic fraction were also followed by the yield of coke, decreasing as long as the polymer/catalyst ratio increased. As mentioned, the yields of coke and the impact on catalyst stability are the matter of a further study.

Since the yields of aromatic hydrocarbons were the highest on the Zn-ZSM-11 zeolite, this catalyst was chosen to study the effect of the reaction temperature on aromatics with a polymer/catalyst relationship of 0.5 and 60 min of reaction time. Fig. 7 shows the influence of this reaction parameter on the C6–C9 aromatic content of the liquid hydrocarbons. It can be seen that the higher the temperature, the higher the aromatic content, approaching 100% at 500 °C, with a liquid yield of approximately 55%. Consequently, the liquid products obtained under these conditions consisted essentially of C6–C9 aromatics only. This trend is consistent with previous observations on the conversion of polyethylene on acidic zeolites [15]. This simplified composition could be of significance because separation and purification steps could be achieved with simpler procedures [35].

Table 5
Product distribution in the conversion of LDPE over Zn-ZSM-11 catalyst. Influence of the polymer/catalyst relationship. Reaction temperature, 500 °C and reaction time, 60 min.

	Yield (wt.%)	
Polymer/catalyst ratio	0.5/1	2/1
Gaseous products	40.06	31.09
C1–C2	4.85	3.53
C3	9.73	9.13
C4	20.78	12.52
C5	3.02	5.03
C6	1.68	0.88
C3–C4 Paraffins/olefins	2.93	2.25
Liquid products	55.12	67.82
C5	0.00	8.31
C6	0.00	16.25
C6–C9 Aromatics	52.98	21.95
C7–C8	1.20	17.62
C9–C10	0.94	3.69
Coke	4.82	1.09

4. Conclusions

It was shown that the catalytic conversion of LDPE over MEL structure zeolites towards the synthesis of hydrocarbons of interest is feasible and constitutes a new and promising option for the tertiary recycling of waste polyolefin polymers. The use of Zn- and H-ZSM-11 zeolites, as opposed to the thermal process, produced more gas and liquid hydrocarbons and less solid residues. However, the yield profiles of Zn- and H-ZSM-11 catalysts differed. The higher yields of gaseous products and the smaller amounts of liquid products in H-ZSM-11 zeolite can be justified on its higher amounts of Brönsted acid sites, favoring cracking reactions; the very high proportion of C6–C9 aromatic hydrocarbons in the liquid fraction observed with Zn-ZSM-11 zeolite is the result of its high concentration of Lewis acid sites, favoring aromatization, that was increased significantly after Zn exchange on the parent zeolite. Depending on experimental conditions, aromatic selectivity in liquid products could be increased to close to 100%. The shape selectivity property of these materials is apparent in the molecular size of the products obtained, and also leads to low coke yields.

Acknowledgements

This project was supported partially by: CONICET-PIP No. 6313/05, FONCYT-ANPCyT-PICT No. 14-14485/03 and UTN-PID 25E092. L.B. Pierella and U. Sedran (researchers) and M.S. Renzini (doctoral fellowship) thank to financial support from CONICET.

References

[1] J. Aguado, D.P. Serrano, "Feedstock Recycling of Plastic Wastes", RSC Clean technology monographs, RSC, 1999.
[2] W. Soroka, Fundamentals of Packaging Technology, IoPP, 2002 ISBN 1-930268-25-4.
[3] APME Association of Plastic Manufacturers in Europe, Summary Report: An Analysis of Plastics Consumption and Recovery in Europe 2002&2003, Brussels, Belgium, 2004.
[4] G. Scott, Polym. Degrad. Stabil. 68 (2000) 1–7.
[5] E.A. Williams, P.T. Williams, J. Chem. Technol. Biotechnol. 70 (1970) 9–20.
[6] N. Kiran, E. Ekinci, C. Snape, Resour. Conserv. Recycl. 29 (2000) 273–283.
[7] K. Fouhy, I. Kim, S. Moore, E. Culp, Chem. Eng. 100 (1993) 30–34.
[8] N. Miskolczi, L. Bartha, G. Deak, B. Jover, Polym. Degrad. Stabil. 86 (2004) 357–366.

[9] E. Hajekova, M. Bajus, J. Anal. Appl. Pyrol. 74 (2005) 270–281.
[10] Y. Kodera, Y. Ishihara, T. Kuroki, Energy Fuel 20 (2006) 155–158.
[11] Q. Zhou, Y.Z. Wang, C. Tang, Y.H. Zhang, Polym. Degrad. Stab. 80 (2003) 23–30.
[12] Y.-H. Lin, M.-H. Yang, J. Anal. Appl. Pyrolysis 83 (2008) 101–109.
[13] Y. Sakata, A. Uddin, A. Muto, J. Anal. Appl. Pyrol. 51 (1999) 135–155.
[14] S. Ali, A. Garforth, D. Harris, D. Rawlence, Y. Uemichi, Catal. Today 75 (2002) 247–255.
[15] R. Bagri, P. Williams, J. Anal. Appl. Pyrol. 63 (2002) 29–41.
[16] L. Pierella, M. Renzini, O. Anunziata, Micropor. Mesopor. Mater. 81 (2005) 155–159.
[17] A.G. Buekens, H. Huang, Resour. Conserv. Recycl. 23 (1998) 163–181.
[18] A. Ayame, Y. Uemichi, T. Yoshida, H. Kanoh, J. Jpn. Petrol Inst. 5 (1979) 280–287.
[19] W. Park, E.Y. Hwang, J.R. Kim, J.K. Choi, Y.A. Kim, H.C. Woo, Polym. Degrad. Stabil. 65 (1999) 193–198.
[20] O. Anunziata, L. Pierella, Catal. Lett. 19 (1993) 143–151.
[21] C.A. Emeis, J. Catal. 141 (1993) 347–354.
[22] M. Schwidder, M. Santhosh Kumar, U. Bentrup, J. Pérez-Ramírez, A. Brückner, W. Grünert, Micropor. Mesopor. Mater. 111 (2008) 124–133.
[23] L. Pierella, C. Saux, S. Caglieri, H. Bertorello, P. Bercoff, Appl. Catal. A: Gen. 347 (2008) 55–61.
[24] J. Zhang, J. Chen, J. Ren, Y. Sun, Appl. Catal. A 243 (2003) 121–133.
[25] G. Busca, Phys. Chem. Chem. Phys. 1 (1999) 723–736.
[26] K. Rhee, U. Rao, J. Stencel, G. Melson, J. Crawford, Zeolites 3 (1983) 387.
[27] R. Borade, A. Sayari, A. Adnot, S. Kaliaguine, J. Phys. Chem. 94 (1990) 5989–5994.
[28] M. Mhamdi, S. Khaddar-Zine, A. Ghorbel, Appl. Catal. A: Gen. 357 (2009) 42–50.
[29] Polymer Data Handbook, Oxford University Press, Inc, 1999.
[30] D. Chen, H. Ling, N. Xu-Wen, W. Xin-Ling, T. Xiao-Zhen, Eur. Polym. J. 39 (2003) 871–876.
[31] R. van Grieten, D. Serrano, J. Aguado, R. García, C. Rojo, J. Anal. Appl. Pyrol. 58–59 (2001) 127–142.
[32] A. Pedroso, D. Rosa, Carbohydr. Polym. 59 (2005) 1–9.
[33] J. Mosio-Mosiewski, M. Warzala, I. Morawski, T. Dobrazanki, Fuel Process. Technol. 88 (2007) 359–364.
[34] J. Abbot, F.N. Guerzoni, Appl. Catal. 85 (1992) 173–188.
[35] K. Takuma, Y. Uemichi, A. Ayame, Appl. Catal. A: Gen. 192 (2000) 273–280.
[36] Cumming, Wojciechowski, Catal. Rev. Sci. Eng. 38 (1996) 101–157.
[37] J. Biscardi, G. Meitzner, E. Iglesia, J. Catal. 179 (1998) 192–202.
[38] O. Anunziata, G. Eimer, L. Pierella, Catal. Lett. 75 (2001) 93–97.
[39] C. Liu, Y. Deng, Y. Pan, Y. Gu, B. Qiao, X. Gao, J. Mol. Catal. A: Chem. 215 (2004) 195–199.
[40] N. Akpanudoh, K. Gobin, G. Manos, J. Mol. Catal. A: Chem. 235 (2005) 67–73.